

Article

Water Distribution Characteristics of Slopes Based on the High-Density Electrical Method

Xiaochun Lu ^{1,2}, Xiao Liu ^{1,2}, Bobo Xiong ^{1,2,*}, Xue Cui ^{3,4}, Bin Tian ^{1,2}, Zhenglong Cai ², Ning Shuang ^{1,2} and Mi Zhou ⁵

¹ Hubei Key Laboratory of Disaster Prevention and Mitigation, China Three Gorges University, Yichang 443000, China

² College of Hydraulic and Environmental Engineering, Three Gorges University, Yichang 443000, China

³ Guangdong No.2 Hydropower Engineering Co., Ltd., Guangzhou 511340, China

⁴ Water Conservancy and Hydropower Construction Engineering Technology Research Centre of Guangdong Province, Guangzhou 511340, China

⁵ State Key Laboratory of Subtropical Building Science, South China Institute of Geotechnical Engineering, South China University of Technology, 381 Wushan Road, Guangzhou 510640, China

* Correspondence: xiongbobo@ctgu.edu.cn

Abstract: Measuring the water content of slopes is essential because the distribution and migration of water within slopes are important factors of landslide instability. In this study, the relationship between the resistivity, volumetric temperature water content and temperature of landslide soil was modelled. The model was validated by indoor landslide model tests and field tests in Baijiabao to investigate the effect of reservoir water levels on the water content of landslide slopes. Test results showed that, as the reservoir levels rose, the water content of the landslide soil increased. Moreover, a good correspondence between the measured results and the inversion results based on the resistivity data was obtained by using the high-density electrical method in combination with the developed model of the relationship between resistivity, volumetric water content and temperature, indicating that the proposed method is reliable and practicable in hydrodynamic landslide monitoring.

Keywords: electrical resistivity; high-density resistivity; landslide; moisture distribution; water condition



Citation: Lu, X.; Liu, X.; Xiong, B.; Cui, X.; Tian, B.; Cai, Z.; Shuang, N.; Zhou, M. Water Distribution Characteristics of Slopes Based on the High-Density Electrical Method. *Water* **2023**, *15*, 895. <https://doi.org/10.3390/w15050895>

Academic Editor: Roberto Greco

Received: 11 December 2022

Revised: 23 February 2023

Accepted: 24 February 2023

Published: 26 February 2023



Copyright: © 2023 by the authors. Licensee MDPI, Basel, Switzerland. This article is an open access article distributed under the terms and conditions of the Creative Commons Attribution (CC BY) license (<https://creativecommons.org/licenses/by/4.0/>).

1. Introduction

Hydrodynamic landslides are slope geotechnical instability hazards driven by hydrodynamic factors, such as glacial snow melting, rainfall, water level changes, surface runoff and groundwater activities [1–5]. Water plays a key role, not only in the shape, movement and disaster-causing processes of landslides, but also in hydrodynamic response, which is closely related to the occurrence of landslide hazards. The official statistics from the Ministry of Natural Resources of China disclose that most landslide hazards are induced by hydrodynamic factors, such as rainfall, water level changes and glacial melting [6–8]. Moisture distribution inside slopes is greatly affected by reservoir water levels, and its response considerably affects landslide instability and failure. Numerous studies have demonstrated that fluctuations in reservoir water levels change the geological environment of bank slopes, resulting in variations in the matric suction of unsaturated soil with the water content of slope bodies and the distribution of moisture inside slopes. This phenomenon generates instability and damage by inducing an unbalanced internal force in slope bodies [9]. If the water level in a reservoir area rises, the pore water pressure and soil pressure within the landslide body also increase. Moreover, the matric suction force decreases; the upper side of the landslide damage area produces tension cracks; the lower side undergoes soil swelling due to the extrusion effect; and the foot of the slope experiences local flow soil and other phenomena. When the water levels of a reservoir landslide change, the internal

seepage field near the average water storage level is frequently disturbed by frequent alternation between wetting and drying, and structure and mechanical strength deteriorate continuously; this effect, in turn, increases the possibility of reservoir landslides [10,11]. Therefore, the corresponding law of water distribution and the migration characteristics of landslides must be studied with regard to hydrodynamic conditions [12].

Given that soil water content affects slope stability, studying its variation is important. The drying method is the most direct and reliable method for measuring moisture content. Although it is widely used because of its facile operation and high accuracy, it is inefficient and difficult to use for long-term monitoring. Amongst field measurement methods, remote sensing [13] is suitable for large-scale water content testing. It has the advantages of a wide monitoring range and high efficiency, and does not damage the soil layer. Nevertheless, its spatial resolution is low and easily disturbed by factors such as topography, vegetation cover and soil roughness, and its measurement technology remains immature. The measurement methods applicable to soil moisture monitoring are time-domain reflection [14–18], frequency-domain reflection [19], the neutron method [20] and the infrared test method. Although each method has its advantages, they all have certain limitations.

The geophysical method is a non-invasive method for site investigation that provides new technical ideas for obtaining the cross-sectional data on soil water content. The high-density electrical method is one of the most important geophysical exploration methods [21], and is based on the electrical method [22–25]. The high-density resistivity method is an array-based exploration method in which the spatial and temporal distribution of resistivity is obtained by laying electrodes in the measured medium and measuring soil resistance [26]. The presence of moisture reduces the resistivity value of different water-bearing media. The high-density electrical method is feasible and advantageous because it can quickly collect geoelectric data over a large area and facilitate a comprehensive understanding of moisture distribution in water-bearing media [27].

Soil grain characteristics, pore characteristics, saturation and temperature are the four main factors affecting soil resistivity [28]. Amongst these factors, water content [29] and temperature [30] are more influential than others. In addition, the stability of hydrodynamic slopes is most influenced by environmental factors, i.e., temperature, and water level, i.e., water content. Thus, establishing a resistivity model based on water content and temperature is important for capturing water level distribution by using high-density electrical methods.

In this study, the Baijiabao landslide was taken as the research object and the relationship of soil resistivity with hydrodynamic slope volumetric water content and temperature was systematically studied by applying high-density electrical measurement technology, combining indoor geotechnical tests, indoor physical model tests and field monitoring, and establishing a resistivity–volumetric water content–temperature relationship model. The model was applied to the field monitoring of the Baijiabao landslide and was verified to be useful for practical application in monitoring water migration within landslides under hydrodynamic conditions.

2. Electric Conductivity Model of the Soil

Establishing the conductivity model of the slope soil by applying the high-density resistivity method is an important task in the measurement of water distribution in slopes. A series of specimens with different parameters were utilized to obtain the electric conductivity model of the soil, and their electrical resistivity was measured.

2.1. Test Scheme

For a certain type of soil, electric conductivity varies in accordance with numerous factors, such as compactness, moisture content, ion type and pore water content and temperature. In this study, the relationship between electrical resistivity, compactness, moisture content and temperature was investigated. Soil can be considered as a three-phase

system consisting of solid, liquid and gas. Thus, porosity n and saturation S_r (%) were used to define the structural characteristics of the specimens. Porosity n reflects the compactness of the soil, and is defined as

$$n = 100 \frac{\rho_w - \rho_d}{\rho_{wat} S_r}, \quad (1)$$

where ρ_w (g/cm^3) is the wet density of the specimen; ρ_d (g/cm^3) is the dry density of the specimen; and ρ_{wat} (g/cm^3) is the density of the water. S_r (%) is the saturation of the specimen, and can be used to describe the volumetric water content ω , which can be expressed as

$$\omega = \frac{n S_r}{100}. \quad (2)$$

Four kinds of specimens were designed with porosities of 0.36, 0.4, 0.44 and 0.48 to build an electric conductivity model of the soil. For each type of specimen, saturation was set to 0%, 40%, 60% and 99%. The resistivity of each specimen was tested at different temperatures, i.e., 10 °C, 20 °C, 30 °C, 40 °C and 50 °C.

2.2. Test Method

The soil used in the experiment was collected from the Baijiabao landslide in the Three Gorges Reservoir area. It is described in detail below. The selected soil had a particle density of $2.75 \text{ g}/\text{cm}^3$ and a natural moisture content of 7.4%. After air drying, grinding, screening and heat drying, the treated soil was stored in a sealed bag.

On the basis of the preset test scheme, a series of specimens was used as illustrated in Figure 1a,b. The test results were based on the average of three test specimens with preset porosity and saturation to reduce test error. A triaxial saturator and a vacuum water dispenser were used, as displayed in Figure 1c, to ensure that the specimen reached a saturation of 100%. A cabinet with constant temperature and humidity was applied to regulate the temperature of the specimen, and the saturation was held constant, as illustrated in Figure 1d.

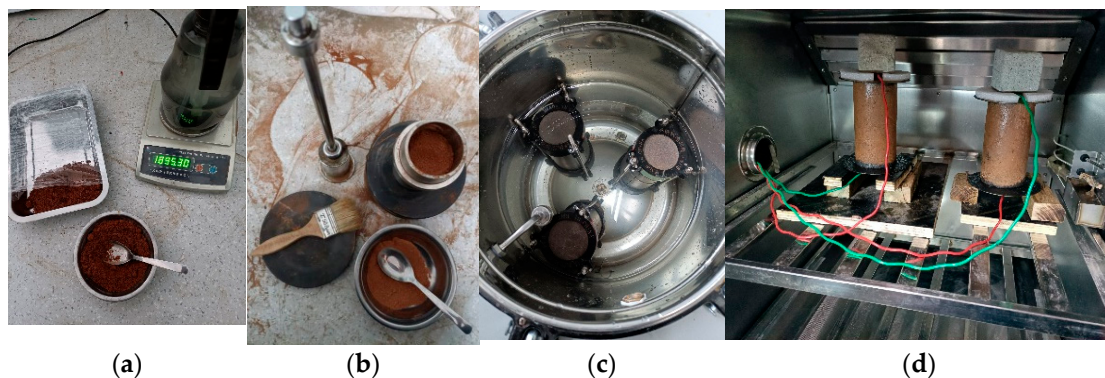


Figure 1. Indoor experiment: (a) soil sample preparation, (b) soil specimen production, (c) saturated specimen and (d) temperature and humidity control.

Figure 2 depicts the two-electrode method used in this study. Through this method, the electrical resistivity of the specimen ρ ($\Omega \cdot \text{m}$) can be expressed as

$$\rho = \frac{US}{IL}, \quad (3)$$

where U (V) is the potential difference between the two sides of the specimen; I (A) is the current flowing through the specimen; S (m^2) is the sectional area of the specimen and L (m) is the length of the specimen. As illustrated Figure 2, conductive paste was painted onto the inner surface of the copper electrode to guarantee measurement accuracy.

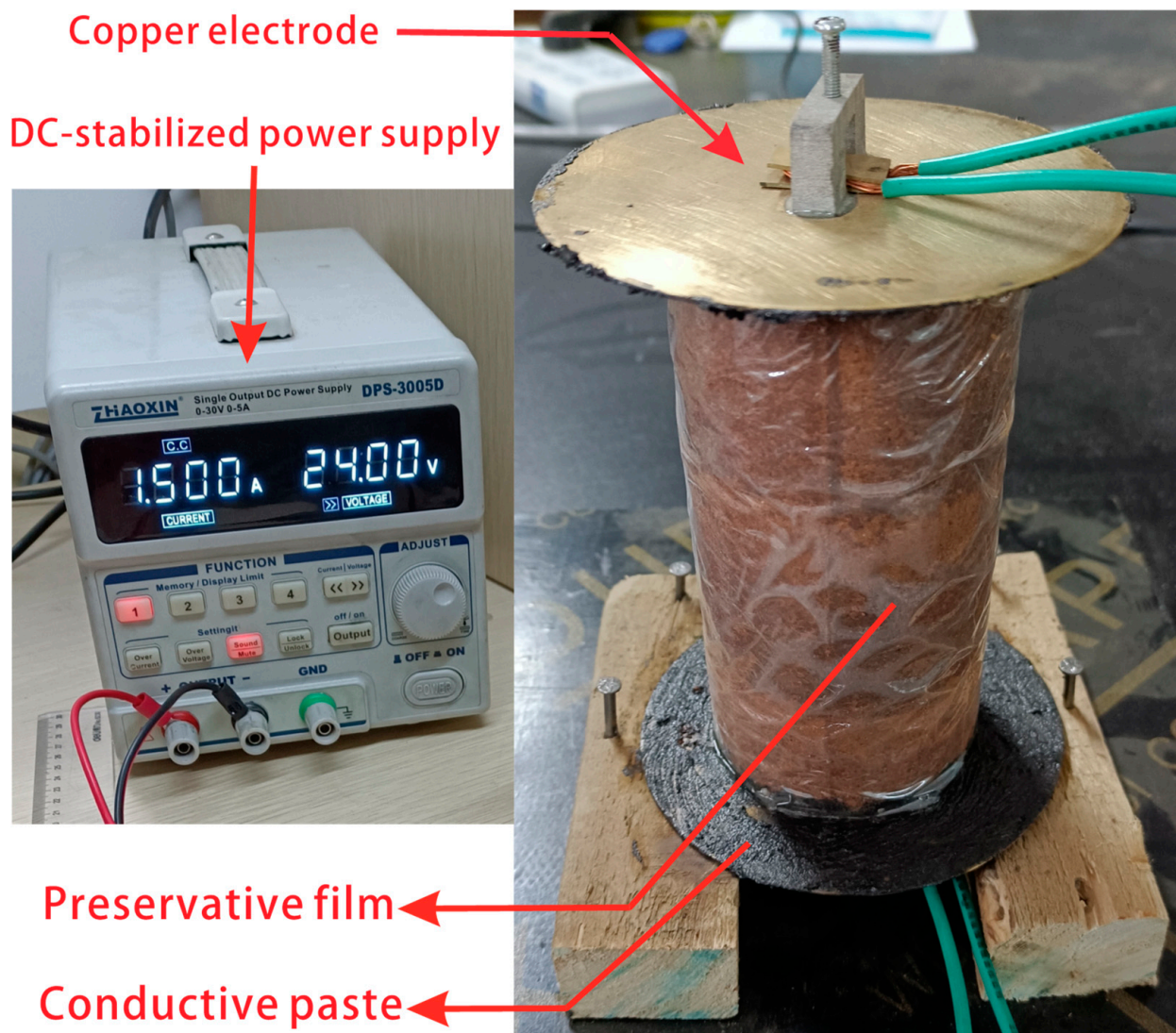


Figure 2. Soil resistivity test with the two-electrode method.

2.3. Results and Analysis

Figure 3 shows that resistivity increased with the increase in porosity, whereas the other conditions did not vary greatly. However, when saturation was high, the effect of the increase in porosity on resistivity was relatively small because the electrical conductivity of the soil was mainly determined by pore water. For the same soil–rock composite media, resistivity decreased considerably with the increase in saturation. Therefore, in this study, porosity and saturation were combined into one index, namely volumetric water content.

Figure 4 presents the influence of volumetric water content and temperature on resistivity. The changes in resistivity under different temperature conditions were approximately the same and were negatively correlated with water content. When the volumetric water content was constant, resistivity decreased with the increase in temperature. When the volumetric water content was less than 25%, resistivity increased rapidly. With the increase in volumetric water content, resistivity changed rapidly due to the good conductivity of the water inside pores. When the volumetric water content exceeded 35%, the resistivity of soil and stone aggregates decreased slowly with the further increase in volumetric water content. When volumetric water content exceeded a certain value, the liquid water within the pores formed a continuous network and the additional liquid water did not greatly reduce the resistivity value of the soil.

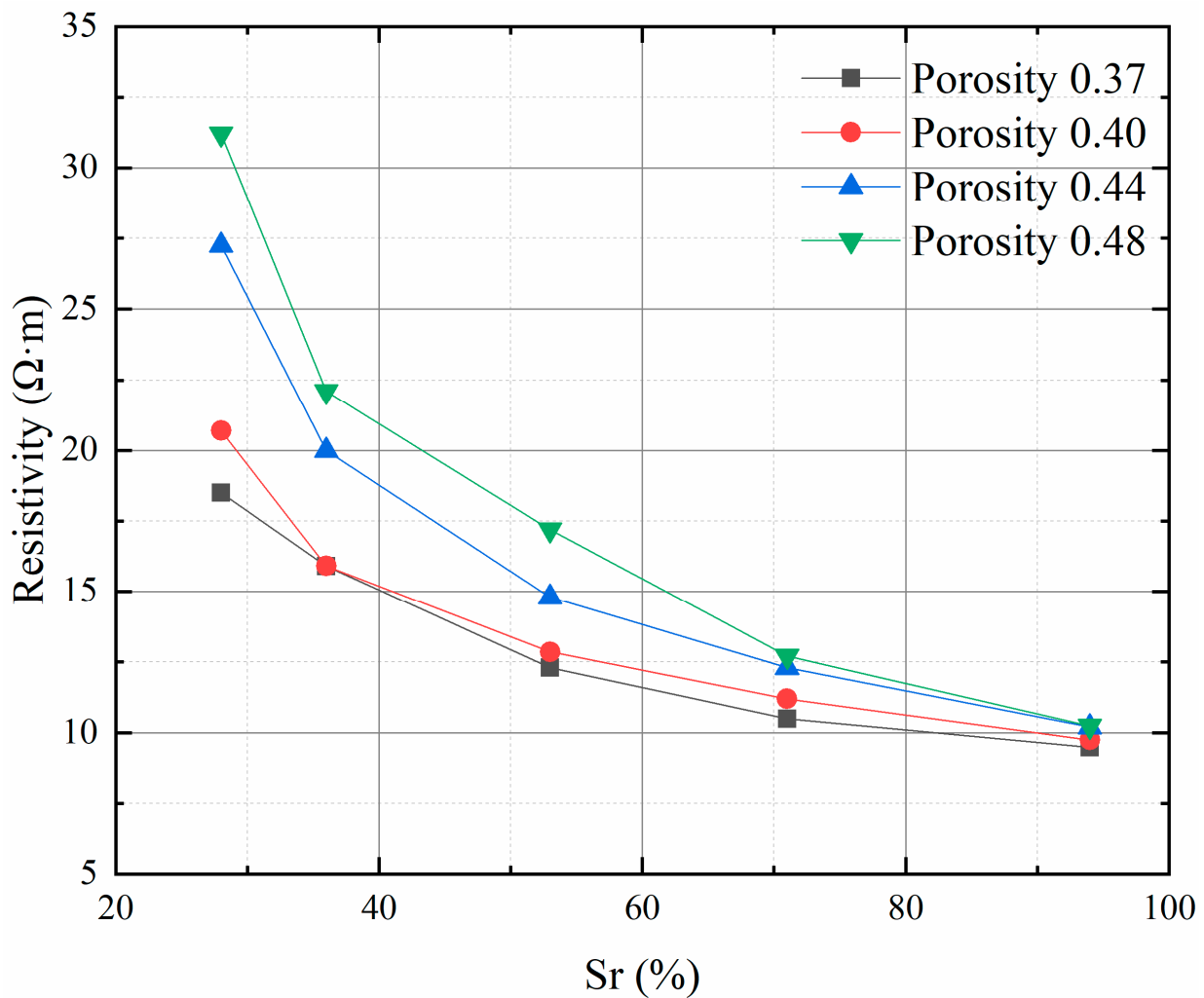


Figure 3. Variation in soil resistivity with saturation.

When the other conditions remained unchanged, resistivity exhibited a regular non-linear change with volumetric water content. Resistivity changed from 50 $\Omega\cdot\text{m}$ to 15 $\Omega\cdot\text{m}$ when the volumetric water content was varied from 0.12 to 0.47 at 10 $^{\circ}\text{C}$. At 50 $^{\circ}\text{C}$, resistivity changed from 23 $\Omega\cdot\text{m}$ to 8 $\Omega\cdot\text{m}$ when the volumetric water content was changed from 0.12 to 0.47. That is, the lower the temperature, the greater the change in resistivity with the change in volumetric water content. When the volumetric water content was 0.12, resistivity changed from 50 $\Omega\cdot\text{m}$ to 22 $\Omega\cdot\text{m}$ with the change in the temperature from 10 $^{\circ}\text{C}$ to 50 $^{\circ}\text{C}$. When the volumetric water content was 0.47, resistivity changed from 17 $\Omega\cdot\text{m}$ to 8 $\Omega\cdot\text{m}$ when the temperature was changed from 10 $^{\circ}\text{C}$ to 50 $^{\circ}\text{C}$. That is, the lower the volumetric water content, the greater the change in resistivity with the change in temperature. Figure 4 shows that, although the resistivity of the specimen had a turning point or even an opposite trend at different water content intervals, the overall trend and resistivity were strongly negatively correlated. Therefore, a reliable model of the relationship between conductivity, volumetric water content and temperature can be established.

2.4. Resistivity Model

Although many studies have been conducted on the relationship between the resistivity of rocks with the soil mass and its different influencing factors, the resistivity of a medium remains complex because it is affected by the physical properties of the soil mass, the chemical composition of the aqueous solution and external temperature. No calculation formula can perfectly reflect these relationships. The influence of the chemical composition

of liquid water on resistivity was not considered in this study. As mentioned above, resistivity has a significant negative correlation with volumetric water content and temperature. In consideration of the factors of volumetric water content and external temperature and in accordance with the above test data, the resistivity of the studied soil–rock aggregate can be expressed as follows and the fitted surface is shown in Figure 5:

$$\Omega = 71.9615 - 134.66918\omega - 1.10565t + 63.46923\omega^2 + 0.00659t^2 + 1.07183\omega t, \quad (4)$$

where Ω is the resistivity value, ω is the volumetric water content and t is the temperature. Comparing the fitted formula with the measured data revealed that the correlation coefficient of the formula was 0.98391, which indicated a high goodness of fit.

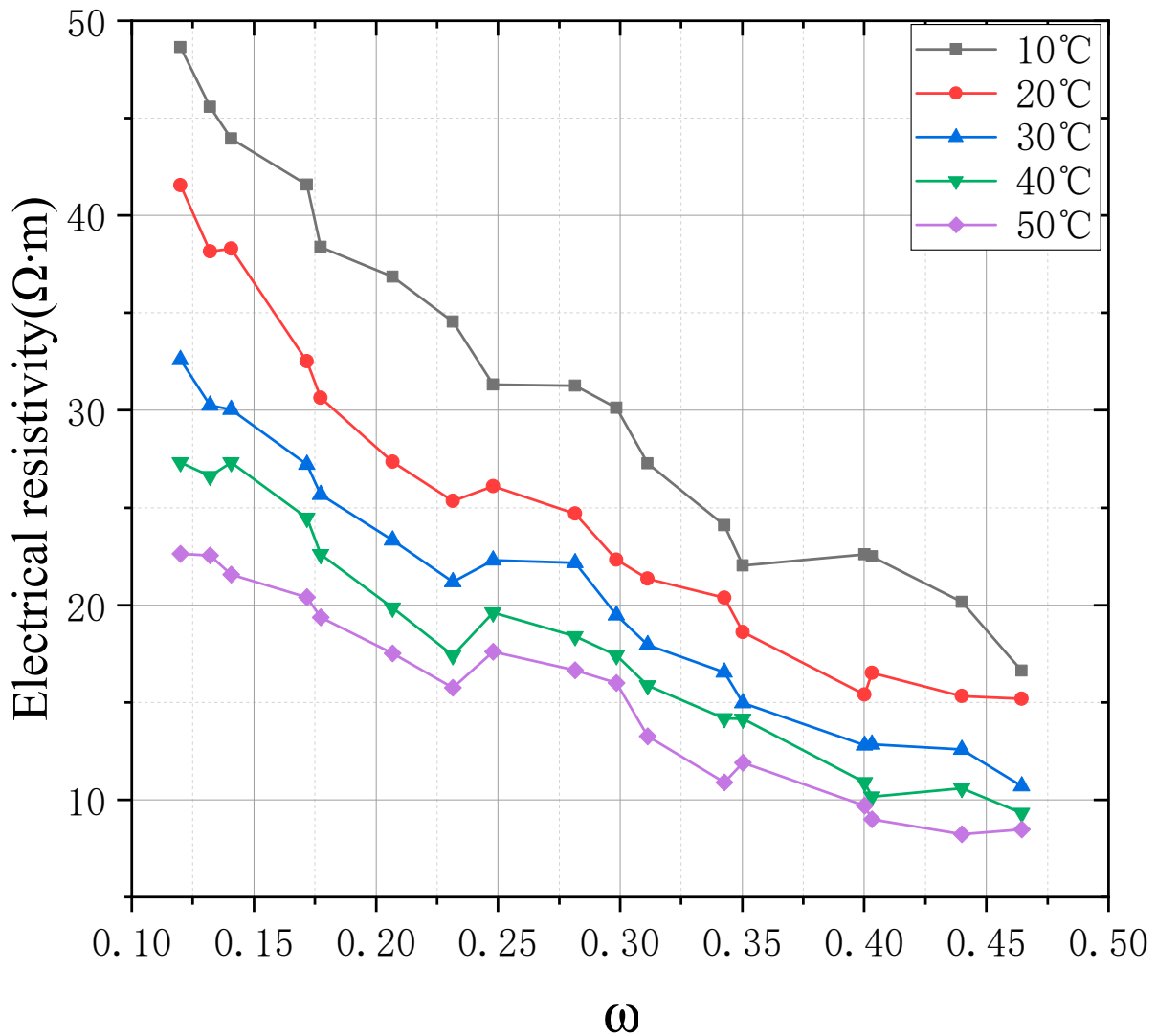


Figure 4. Variation in resistivity with water content under different temperature conditions.

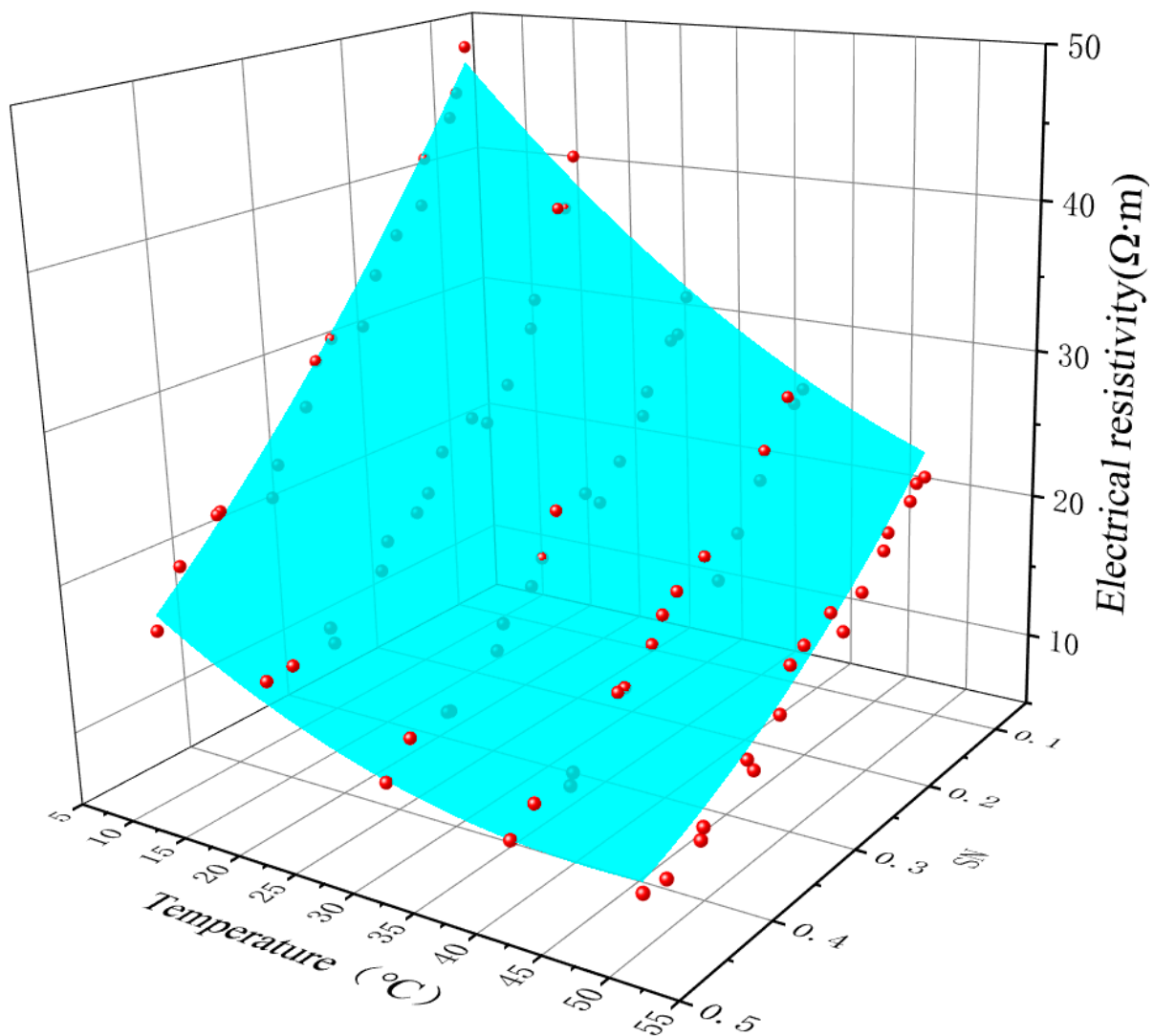


Figure 5. Graph of the volumetric water content–temperature–resistivity relationship.

3. Large-Scale Landslide Indoor Model Test

A large-scale landslide model test was conducted to verify the reliability of the obtained resistivity model. The landslide model was applied to investigate the migration characteristics of slope water under two hydraulic conditions: changes in water level in front of the slope and rainfall. Water content, pore water pressure and resistivity, which can reflect the soil state, were measured during the test.

3.1. Construction of the Model Test

Figure 6 shows that the landslide model was built on a special test platform, which was 8 m long, 2 m wide and 3.5 m high. A water supply pipe and a drainage pipe, which could control the water level at the front of the slope, were located at the left end of the test platform. A series of nozzles were installed on top of the test platform to simulate different rainfall intensities.

The material of the landslide body was the same as the material used in the resistivity test, and the initial material parameters were the density γ of 1.7 g/cm³ and moisture content ω of 15%. The tamping method was used to build the landslide model with respect to operability. The thickness of the filling level and the number of hammers were strictly controlled to ensure that the material in different parts of the landslide model had the material properties specified in Table 1.



Figure 6. Platform for the landslide model test.

Table 1. Material properties of the landslide body.

Name	Initial Volumetric Water Content	Initial Density
Landslide body	15%	1.7 g/cm ³

Soil moisture sensors were installed in the landslide model, and Figure 7 illustrates the soil moisture pressure sensors arranged in four sections. The high-density resistivity method, the main measurement method in this experiment, was applied to the landslide model, and electrode bars were inserted into the surface of the landslide with a horizontal interval of 0.2 m. The sensors and measuring equipment used are shown in Figure 8. The soil moisture (water content) sensor was a product developed by Laiende Intelligent Technology Ltd., and its technical parameters are specified in Table 2.

Table 2. Technical parameters of the soil moisture sensor.

Model Specification	LD-EC
Signal Output Type	RS485 interface, Modbus protocol
Measuring Range	0–100%
Accuracy	3%
Operating Environment	−40–85 °C
External Dimensions (mm)	45 × 15 × 145

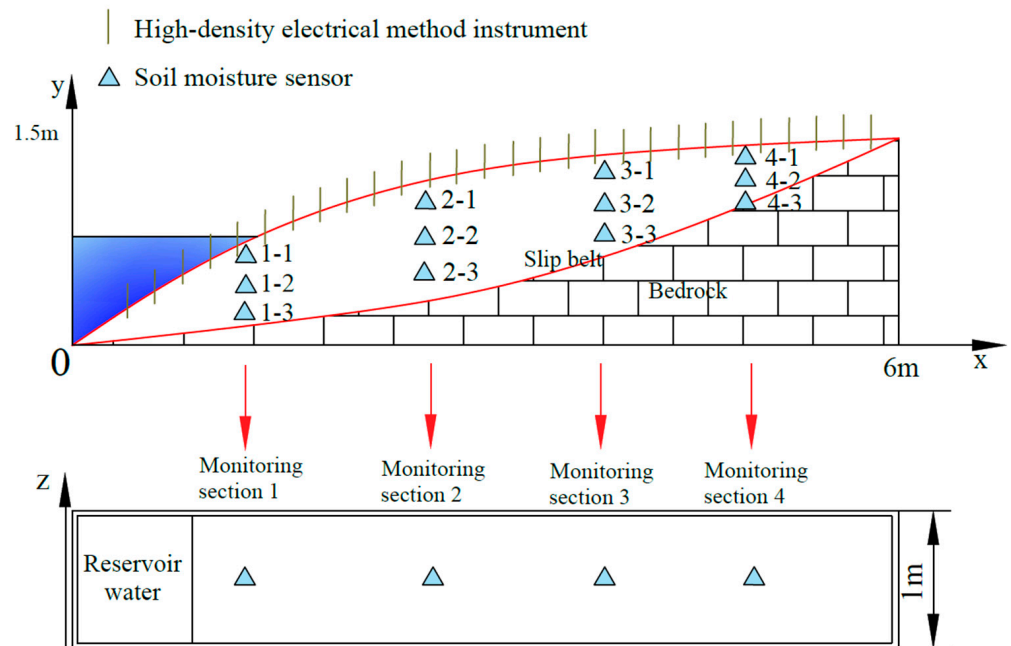


Figure 7. Layout of the model’s physical monitoring points.



Figure 8. Monitoring instrument: (a) LD-EC soil moisture sensor, (b) DZD-8 multifunctional full-waveform DC electrostatic instrument.

3.2. Hydraulic Conditions

Reservoir water levels are an important hydrodynamic condition of reservoir slopes. They can result in displacements and affect slope stability. In this experiment, four water levels were used. The specifications of water levels and durations are displayed in Figure 9. The influence of rainfall was also studied in the experiment. The rainfall duration was 24 h, and the rainfall intensity was set to 0.29 and 0.25 mm/min. These two important hydraulic conditions were simulated in the landslide model, and their responses were tested and analyzed in detail.

3.3. Test Results

Data on the resistivity, temperature and volumetric water content of the landslide body were obtained from indoor model experiments on the landslide. Then, the predicted volumetric water content of the landslide body was inverted by using the previously specified resistivity equation in combination with the experimentally obtained resistivity and temperature data. Monitoring data taken over 60 h of the rising phase of the reservoir water levels were selected for calculation and analysis to verify the correctness of the above resistivity model. The resistivity and temperature values at the exact locations of the sensors were selected for inverse analysis to correspond to the actual monitoring data on water content on a case-by-case basis.

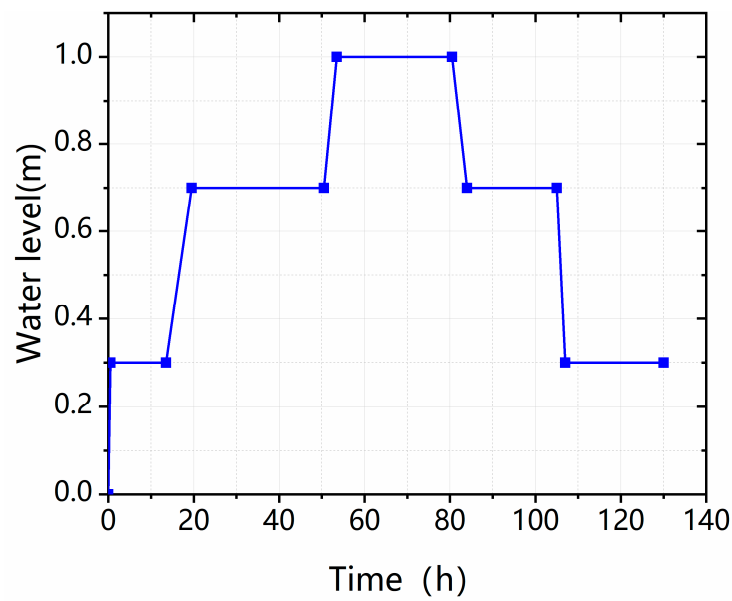


Figure 9. Curve of the regulation of the reservoir water level.

The actual measured volumetric water content of the landslide model ranged from 5% to 50% within the design conditions of the laboratory test, and the soil water content of the landslide gradually increased as the water levels of the reservoir rose and water gradually infiltrated the landslide during the rising phase of reservoir water levels.

As shown in Figure 10, a slight difference was found between the values of volumetric water content obtained from the equations fitted in this study and the actual monitored volumetric water content. Moreover, the predicted values were distributed around the actual monitored values, and the root mean square error of the model was only 0.0211. Therefore, the inversion of the resistivity model is suitable and has a certain reliability.

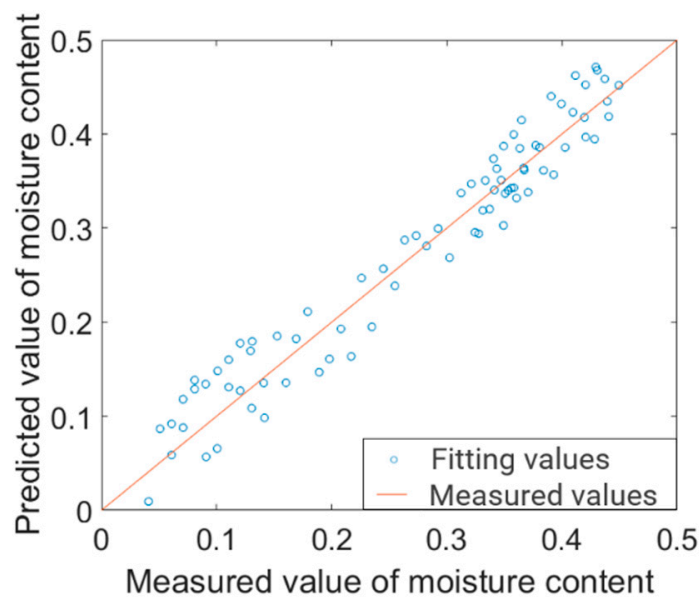


Figure 10. Fitting curves of specimens with saturation.

4. Field Experiment

4.1. Brief Introduction to the Baijiabao Landslide

4.1.1. Spatial Morphology and Material Composition of the Baijiabao Landslide

The Baijiabao landslide is located in Group 2 of Xiangjiadian Village, Zigui County, in the Three Gorges Reservoir area on the right bank of the Xiangxi River, which is a tributary of the north bank of the Yangtze River. It is 2.5 km away from the Xiangxi Estuary and 41.2 km away from the Three Gorges Dam site. Its geographical coordinates are $30^{\circ}58'59.9''$ N, $110^{\circ}45'33.4''$ E. The slope body wherein the landslide is located has a gentle platform slope and gully ridge, and its terrain varies greatly. The strata in this area are dominated by Jurassic sand and mudstone. Given that the study area is located in the western Hubei fold mountain, the terrain gradient changes considerably. The valley area, low hill area and middle alpine denudation mesa terrain slope are slow and are typical erosion structure types. The landslide had no obvious surface macrodeformation characteristics before the Three Gorges Reservoir was impounded in 2003, but began to show signs of deformation after the impoundment. A realistic view of the Baijiabao landslide feature is shown in Figure 11.

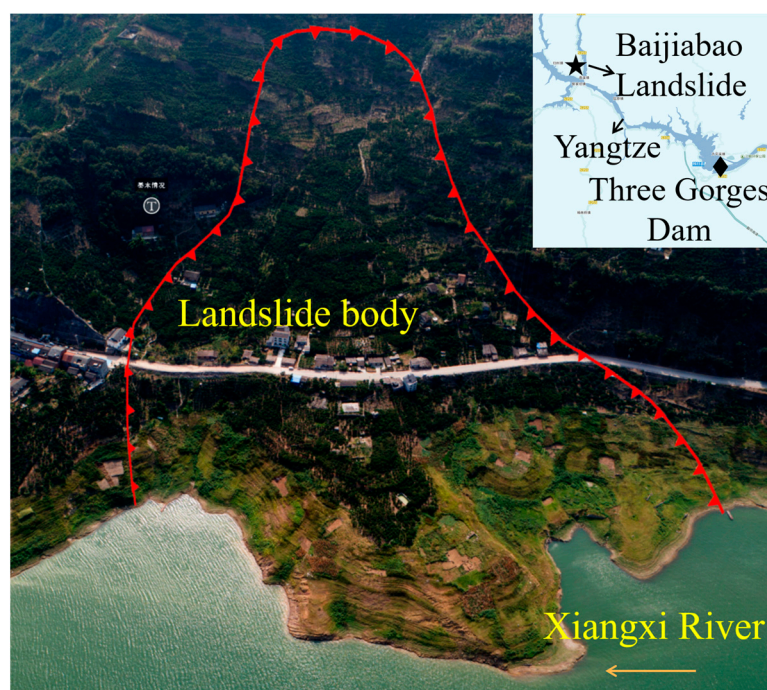


Figure 11. Baijiabao landslide.

The Baijiabao landslide is a typical landslide soil accumulation. Its back edge is bound by a steep and slow intersection on the landform. The Baijiabao landslide has a trend of approximately 40° , and its back edge has an elevation of approximately 270 m. The left and right sides of the landslide are bound by a protruding ridge with exposed bedrock on both sides. The right side of the ridge reaches 85° . The leading edge runs straight to the Xiangxi River, with an elevation of approximately 125 m. The landslide is narrow from top to bottom, with an average width of approximately 400 m. Its leading edge is approximately 500 m wide, its trailing edge is approximately 300 m wide and its longitudinal length is approximately 550 m. The landslide accumulation body has an average thickness of 35 m. The landslide body has a surface volume of $24 \times 10^4 \text{ m}^2$ and a volume of $840 \times 10^4 \text{ m}^3$ as shown in Figure 12. Geomorphologically, the front part of the landslide is convex and falls into the Xiangxi River with an average slope of approximately 20° ; the middle part is relatively gentle and is approximately 10° – 15° and the rear part is steep. The landslide is a typical reverse slope with a concave profile. The material composition of the landslide is mainly landslide deposits comprising grey–yellow and brown–yellow silty clay and

irregularly alternating intercalated gravel and fragmentary stone soil. The silty clay is loose to slightly dense, hard plastic to plastic and slightly wet, and the block stone is mainly composed of strong to moderately weathered sandstone and mudstone with a fragment content of 5–50% and a particle size of 0.2–60 cm. The gravel soil is slightly dense to dense. The stone content can reach 30–50%, and the fine soil contains silty clay, clay and breccia.

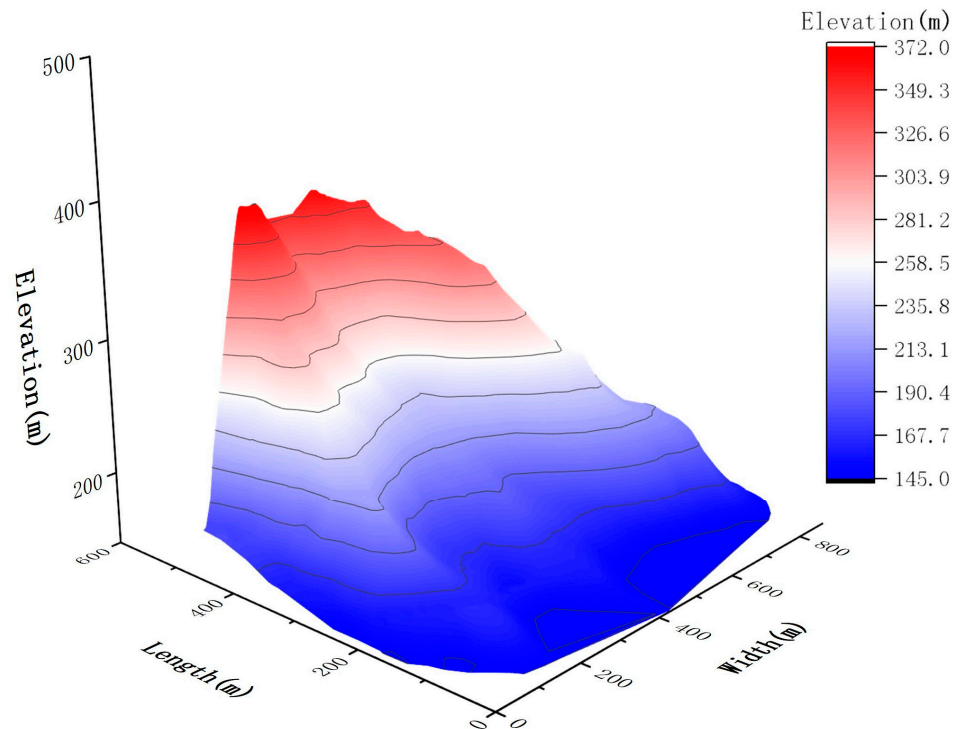


Figure 12. Three-dimensional morphology of the Baijiabao landslide.

4.1.2. Analysis of the Genesis Mechanism of the Baijiabao Landslide

A strong correlation was observed amongst landslides, water storage and rainfall. Although the water stored in the reservoir is insufficient to cause landslide damage, it often induces deformation and numerous surface cracks. This condition allows the enrichment and migration of surface water in the landslide body, and rainwater enters the slope surface along the cracks, reducing the shear strength of the soft ground surface and thus promoting landslide sliding damage. The Baijiabao landslide was caused by numerous cracks on the surface of the back edge and both sides of the edge of the landslide. Under continuous rainfall, rainwater poured into the cracks, resulting in severe deformation.

As depicted in Figure 13, after the completion of the Three Gorges Dam, the rapid rise of the water level of the Xiangxi River from approximately 70 m to 145 m resulted in the submergence of part of the geotechnical body by the reservoir water. The immersion effect of the water changed physical and mechanical properties. Continuous rainfall generated cracks in the ground surface. When rainwater infiltrated these cracks, the moisture distribution inside the slope level increased, the landslide materials became soaked and softened, and siltation occurred. Shear strength then decreased, resulting in damage to the reservoir bank slopes and landslide deformation. Therefore, fluctuations in reservoir water levels and rainfall are the main factors of landslide deformation. In addition, river erosion at the leading edge of the landslide, the formation of open surfaces and the road truncation of the slope indirectly contributed to the revival of the landslide.

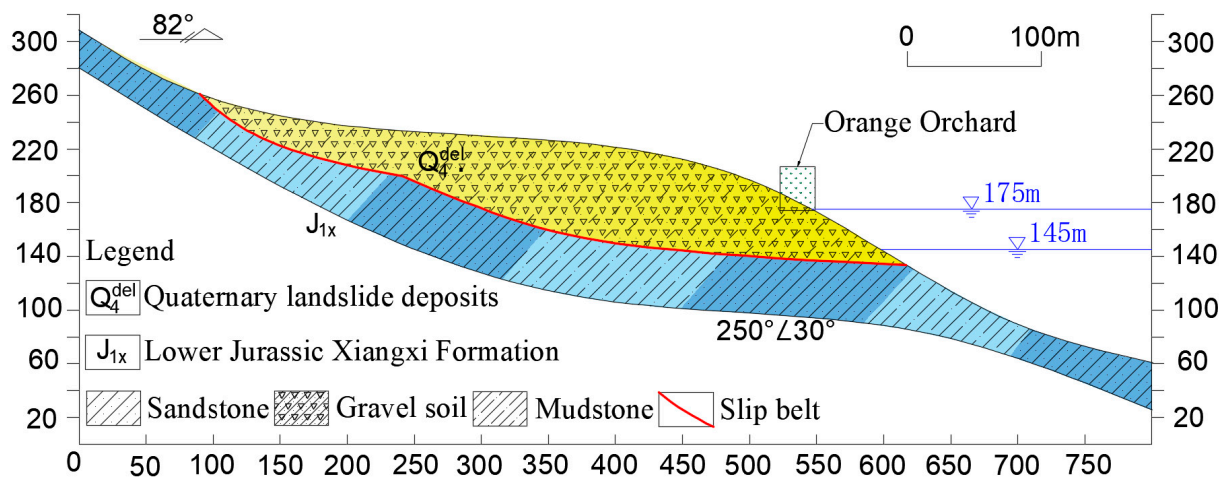


Figure 13. Longitudinal profile of the Baijiabao landslide.

4.2. Measurement Scheme

The Baijiabao landslide soil body was surveyed by using the high-density electrical method to monitor its moisture content distribution during fluctuations in reservoir water levels and verify the feasibility of the resistivity model for practical engineering. As shown in Figure 14, high-density electrical method instruments were arranged along four survey lines on the landslide body. The numerical position in the figure is the starting point of the measurement. A soil moisture sensor and the drying method were used to obtain the true value of the water content of the landslide body on the basis of samples drilled at the intersections of the survey lines. A soil moisture thermometer was utilized to measure the temperature of the soil body at different depths. The instrument arrangement of the high-density electric method was as follows: The longitudinal electrode spacing was set to 2 m, the wiring length was 40 m and 20 electrodes were arranged in accordance with the Wenner α mode. The horizontal electrode spacing was 1 m, the wiring length was 20 m and 20 electrodes were arranged in accordance with the Wenner α mode.



Figure 14. Layout of the high-density electrical survey line of the Baijiabao landslide.

Firstly, the starting point was determined to be as close as possible to the Xiangxi River to ensure safety as shown in Figure 15. Then, a tape measure was employed to determine the position of the electrical instrument and the electrodes were aligned in a straight line. After inserting an electrode rod into the soil, the electrode wire was connected without a power supply. The instrument was turned on for measurement after the measuring lines and points of the high-density electrical instrument were arranged. Given the high input voltage, no one was allowed near the electrode during measurement. The measurement conditions were the variations in the reservoir level, as shown in Table 3.



Figure 15. Field work in Baijiabao landslide.

Table 3. Reservoir water levels during measurement.

	Real-Time Reservoir Water Level (m)
First measurement	168.11
Second measurement	168.26
Third measurement	168.40
Fourth measurement	168.67

Borehole sampling with a Luoyang shovel was performed at the intersection of the transverse and longitudinal survey lines (Figure 16) to test the reliability of the predicted results. Each sampling hole was divided into layers with an interval of 0.5 m. Three soil samples were taken with a ring knife, and each hole was divided into six layers with a depth of 3 m. Each soil sample was treated on the same day and weighed to determine its mass and volume. A microwave oven was used to dry the soil sample. Then, the soil sample was weighed to determine its quality and calculate its water content.



Figure 16. Drilling and sampling.

4.3. Results and Analysis

As depicted in Figure 17, the distribution of resistivity values at the four lines of the landslide field test was obtained by using the electrical inversion software RES2DINV on the basis of the least squares method. The resistivity of the landslide soil at survey lines one and two had distinct horizontal and vertical spatial distribution characteristics. In the vertical direction, the surface layer of the landslide soil was a low-resistance area because the reservoir water was in a rising phase for a week before the monitoring and the surface soil was washed by water. High resistance was found below the surface of the low-resistance area to the monitoring boundary because the landslide soil is a multiphase composite soil–rock mixture with a large amount of disordered soil and rocks, and the deeper soil had high resistance when it was not infiltrated by seepage from the reservoir water. In the horizontal direction, the area close to the reservoir water location was a low-resistance area. During the rising phase of the reservoir water, the reservoir water recharged and percolated into the landslide soil body. The water content of the landslide soil increased, and the resistivity value accordingly decreased. The increase in the soil resistivity value at the area away from the reservoir water reflected the migration path of the soil water.

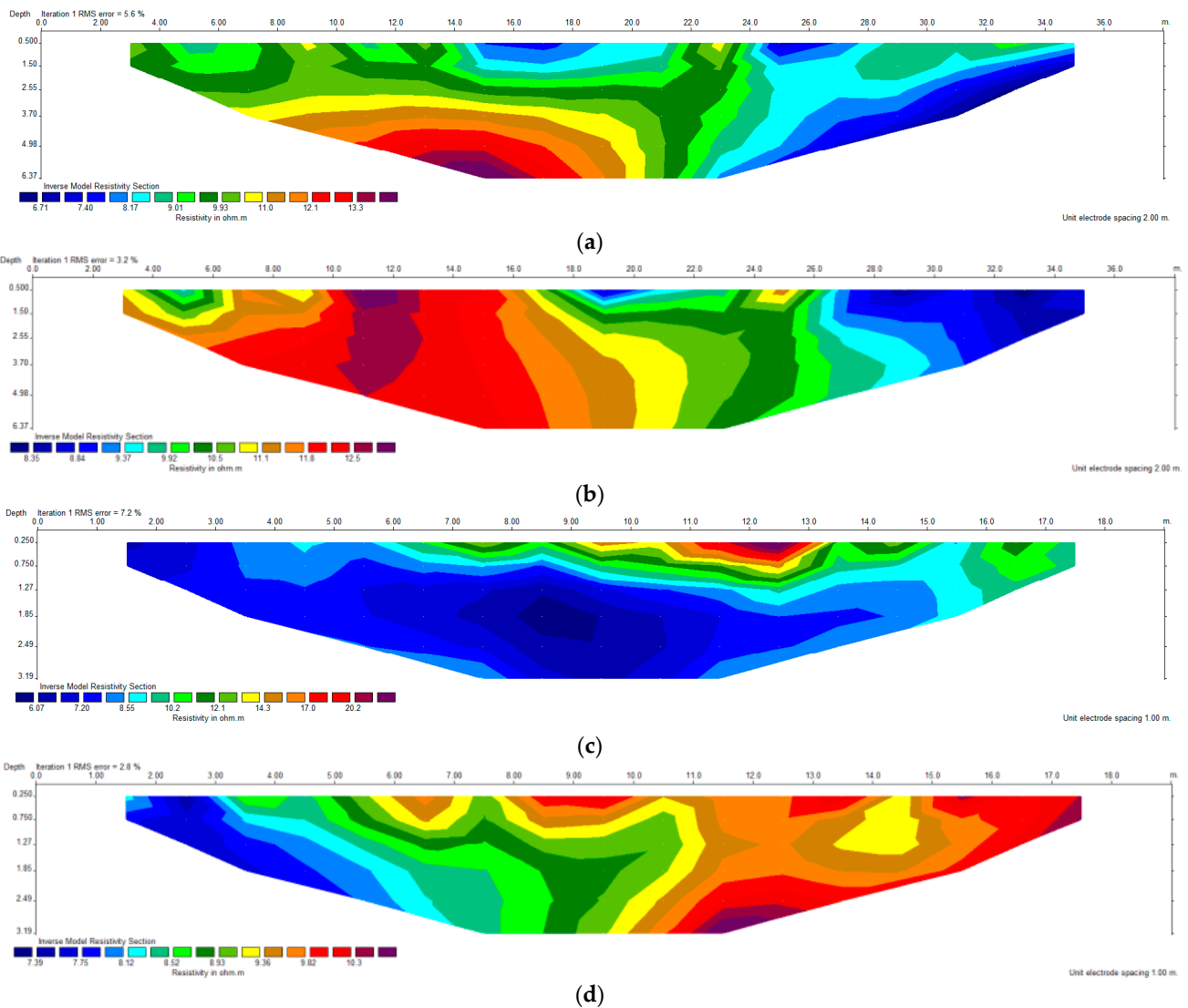


Figure 17. Resistivity distribution of different measuring lines: (a) survey line 1; (b) survey line 2; (c) survey line 3; (d) survey line 4.

At survey lines three and four, the horizontal differences in the distribution of the resistivity of the landslide soil were more significant than the vertical differences. Both survey lines in the area near the reservoir water represented a low-resistance area. The resistivity at line three increased steeply at 12 m, which is a rocky area in accordance with the site survey, and increased in the vertical direction at 0.8 m from the soil surface, presumably due to groundwater infiltration into the soil. This phenomenon was also corroborated by the site borehole test, which found that groundwater was present in the borehole at 0.8 m. The smaller resistivity at 2 m than at 18 m indicated that the coefficient of permeability of the landslide was high near the upstream of the Xiangxi River. In this area, the reservoir water had a rapid infiltration rate and extensive infiltration range.

Figure 18 shows that, at locations distant from the reservoir surface, the soil moisture content decreased with the increase in depth because it was located far from the reservoir water. Moreover, the degree of the influence of reservoir water fluctuation gradually decreased. At locations near the reservoir surface, the soil water content increased with depth because under the condition in which reservoir water levels rose, the water slowly infiltrated upward from the bottom. Moreover, given that the Baijiabao landslide has low permeability, the water had limited ability to percolate and move at great depths. Although the water content values at all four survey lines were larger at the near-water end than at the far-water end, the difference was small. The difference in water content between the two ends of the survey line near the water surface was approximately 10%. The difference in water content between the two ends of the survey line far from the water surface was within 6%. With time, the water content at the far end changed negligibly and that at the near end increased slowly. The water contents at the near ends of survey lines 1, 2 and 3 all increased from approximately 40% to approximately 42%, and the overall water contents at survey lines 1 and 3 were higher than those at survey line 2. Survey line 4 was farther away from the water surface than the other three lines, and the water content at its near-water end increased by <0.5% from approximately 35% to less than 36%.

No rainfall occurred during the week before and during the monitoring period, and the water content data obtained from monitoring predictions were unaffected by rainfall conditions, and all resulted from fluctuations in reservoir water level.

The moisture content data at drill points were obtained by using the traditional drying method. Table 4 shows that volumetric water content varied within the range of roughly 4% with the increase in the depth of the two boreholes at the far-water end of points a and b, and in the range of approximately 6% with the increase in the depth of the two boreholes at the near-water end of points c and d. The volumetric water contents at point a ranged from 33.3% to 37.2%, those at point b ranged from 30.6% to 34.9%, those at point c ranged from 37.8% to 43.0% and those at point d ranged from 36.8% to 42.1%. The temperature varied widely from the surface to the interior of the landslide soil, from 32 °C to 22 °C with the increase in depth, whereas the temperature difference was small at the same depth at different boreholes. Therefore, the temperature at different depths is a significant factor.

Table 4. Volumetric water content and temperature at drilling points.

Location	1 m	2 m	3 m	4 m	5 m	6 m
a	33.30%	33.64%	34.34%	35.27%	36.10%	37.13%
b	30.69%	31.59%	32.51%	33.15%	34.20%	34.83%
c	37.82%	38.40%	39.32%	40.72%	41.55%	42.94%
d	36.88%	38.03%	39.20%	39.62%	40.81%	42.07%
Temperature	32 °C	28 °C	27 °C	25 °C	24 °C	22 °C

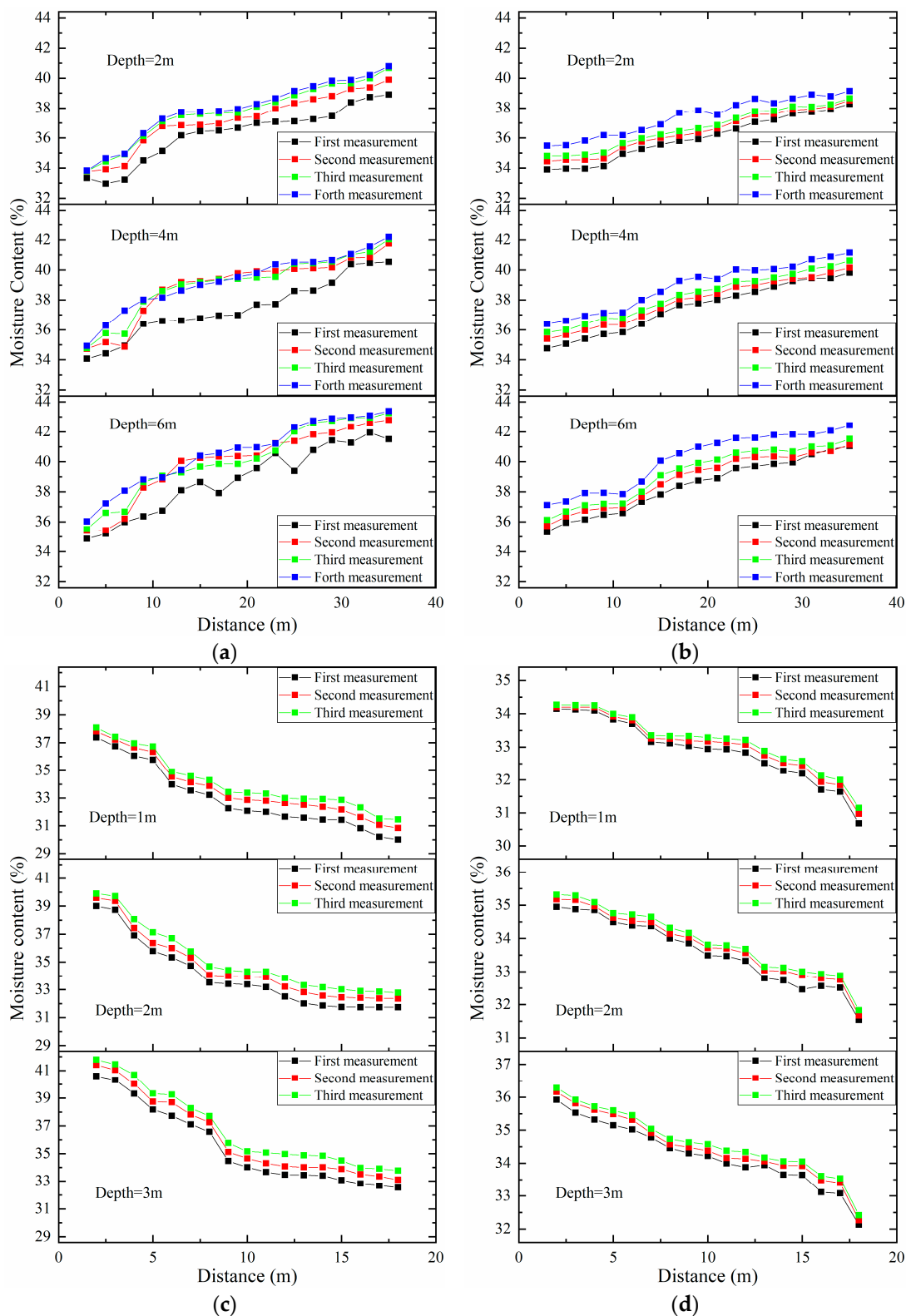


Figure 18. Results of water content inversion: (a) survey line 1; (b) survey line 2; (c) survey line 3; (d) survey line 4.

The data corresponding to borehole locations were selected for comparison and verification to determine the accuracy of the inversion data from the high-density electrical method and the proposed hybrid model for the Baijiabao landslide field test. As shown in Figure 19, the measured values of water content at borehole locations and the inversion

values of the proposed method presented the same trend. The fluctuation in the predicted values above and below the actual values indicated the absence of overall over- or underestimation. The mean-square error value between the two values was 0.346 with an R2 of 0.9706. This result was indicative of a small difference between the inversion and measured values of the model.

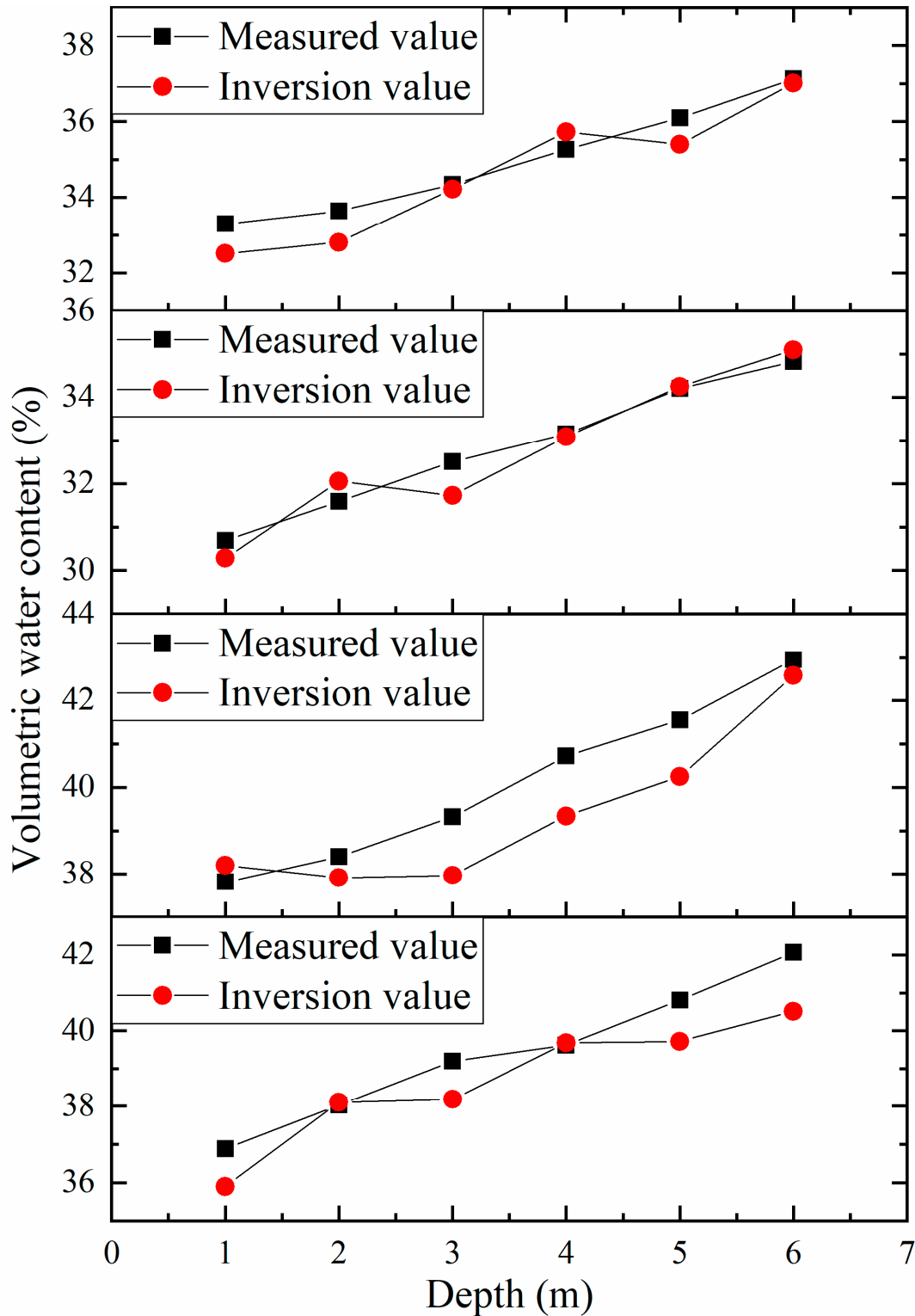


Figure 19. Comparison of the measured and inversion values of volumetric moisture content.

Amongst the four measurement lines at the landslide site, two vertical lines (one and two) were measured four times with the change in reservoir water level, and two horizontal lines (three and four) were measured three times with the change in reservoir water level. The water content contour map of the landslide soil obtained from the prediction of the four survey lines was plotted, as shown in Figure 20.

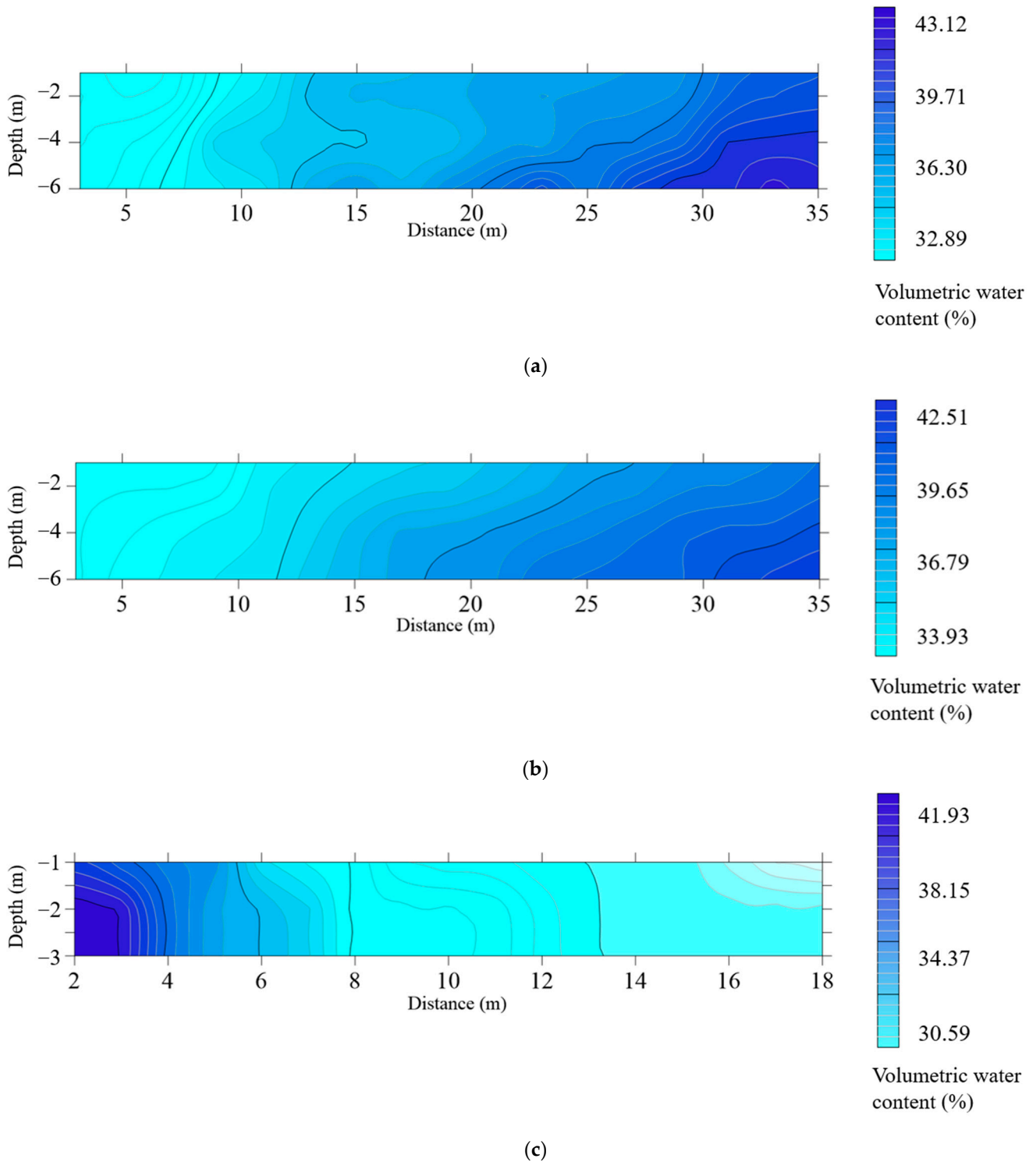


Figure 20. Cont.

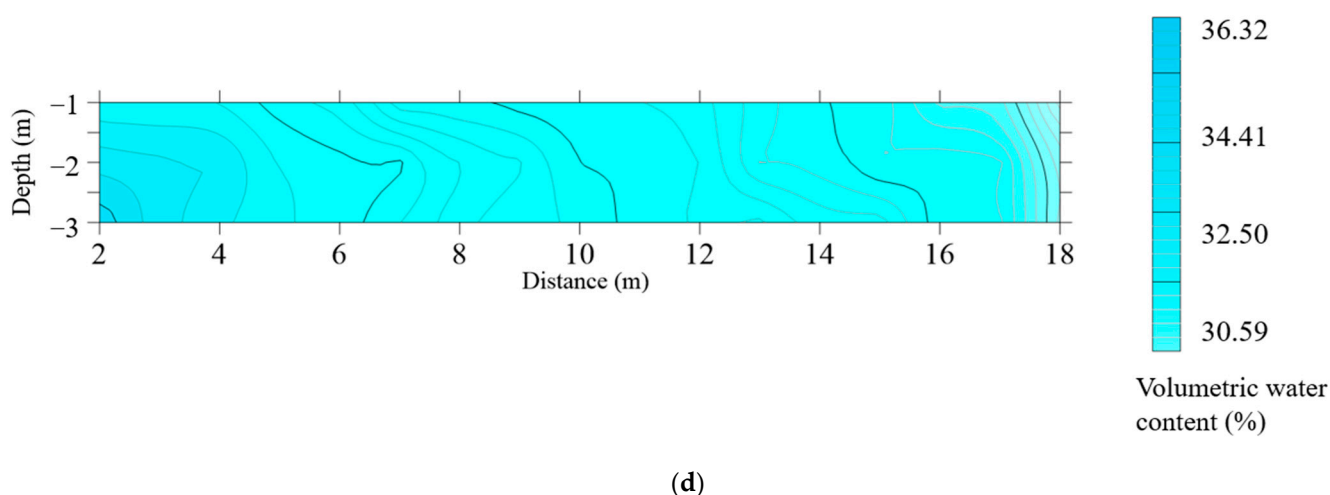


Figure 20. Distribution of the moisture contents of different measuring lines: (a) survey line 1; (b) survey line 2; (c) survey line 3; (d) survey line 4.

For survey lines one and two, the volumetric water content was larger at the location closer to the reservoir surface and gradually decreased as the distance from the water surface increased. Similar results were found for survey lines three and four; given that both ends of survey line four were far from the water surface, the water content profile of survey line four changed nominally. The water content of line three near the reservoir gradually decreased from left to right and changed more than that of line four, indicating that the landslide was near the upstream Xiangxi River with a large permeability coefficient. The reservoir water gradually penetrated the landslide body, and the permeability coefficient gradually decreased in the downstream direction with a slow permeability rate. Similarly, comparing survey line one with survey line two revealed that the moisture content values of survey line one were greater overall than those of survey line two. These findings confirmed the above conclusions.

5. Conclusions

The relationship between resistivity and volumetric water content and temperature was quantified through an indoor geotechnical test, and a resistivity model was constructed. Then, an indoor landslide model test was established to verify the accuracy of the established model. Finally, the Baijiabao landslide was tested by using high-density electrical measurements. The water content distribution in the Baijiabao landslide was derived on the basis of the inversion of the above resistivity model, and the distribution characteristics of water content in response to the change in reservoir level were analyzed. The following conclusions were drawn:

1. Resistivity is considerably correlated with water content and temperature. Given that temperature is not correlated with water content, dry density and pore ratio and affects only the change in resistivity, it is one of the parameters that must be considered. Hence, in this study, volumetric water content and temperature were selected for the study of resistivity, and a resistivity model was established.
2. The model of the relationship of resistivity with volumetric water content and temperature can be used to monitor moisture distribution within slopes under hydrodynamic conditions.
3. The characteristics of water migration in slopes under complex hydrodynamic conditions were investigated. The water content in the landslide soil close to the reservoir were found to rise and reach saturation rapidly as the reservoir's water level rose. The water content of the landslide soil responded slowly with the increase in reservoir water levels. The water content of the landslide soil changed with a certain lag time only after the water level rose further. Furthermore, the lag increased with the

distance from the reservoir. Hysteresis was evident with the increase in the water level position.

Author Contributions: Project administration, funding acquisition, X.L. (Xiaochun Lu); writing—original draft, writing—review and editing, X.L. (Xiao Liu); conceptualization, resources, B.X.; formal analysis, X.C.; data curation, B.T.; methodology, Z.C.; investigation, N.S.; validation, M.Z. All authors have read and agreed to the published version of the manuscript.

Funding: This work was supported by the Hubei Key Laboratory of Disaster Prevention and Mitigation (China Three Gorges University) under Grant No. 2020KJZ10; Hubei Provincial Engineering Research Center of Slope Habitat Construction Technique Using Cement-based Materials (China Three Gorges University) under Grant No. 2022SNJ15; the National Natural Science Foundation of China under Grant No. U2240221; and the National Natural Science Foundation of China (Nos. 52009068, 52109158).

Institutional Review Board Statement: Not applicable.

Informed Consent Statement: Not applicable.

Data Availability Statement: The original contributions presented in the study are included in the article. Further inquiries can be directed to the corresponding author.

Acknowledgments: The authors appreciate KGS for their linguistic assistance during the preparation of this manuscript.

Conflicts of Interest: The authors declare no conflict of interest.

References

1. Tang, M.; Xu, Q.; Huang, R. Types of Typical Bank Slope Collapses on the Three Gorges Reservoir. *J. Eng. Geol.* **2006**, *14*, 172–177. [CrossRef]
2. Xu, Q.; Bai, J.; Tang, M.; Huang, R. Physical Modelling for Examination of Bank Collapse in Three Gorges Area. *J. Eng. Geol.* **2007**, *15*, 154–158. [CrossRef]
3. Liu, L.; Yin, K. Analysis of Rainfall Infiltration Mechanism of Rainstorm Landslide. *Rock Soil Mech.* **2008**, *29*, 1061–1066. [CrossRef]
4. Au, S.W.C. Rain-Induced Slope Instability in Hong Kong. *Eng. Geol.* **1998**, *51*, 1–36. [CrossRef]
5. Chen, M.; Lv, P.; Zhang, S.; Chen, X.; Zhou, J. Time Evolution and Spatial Accumulation of Progressive Failure for Xinhua Slope in the Dagangshan Reservoir, Southwest China. *Landslides* **2018**, *15*, 565–580. [CrossRef]
6. Ministry of Natural Resources of the People's Republic of China. National Geological Disaster Bulletin. 2014. Available online: http://www.cgs.gov.cn/xwl/ddyw/201603/t20160309_299193.html (accessed on 20 January 2015).
7. Ministry of Natural Resources of the People's Republic of China. National Geological Disaster Bulletin. 2015. Available online: http://www.cgs.gov.cn/nb_4906/201507/t20150730_405761.html (accessed on 6 February 2016).
8. Ministry of Natural Resources of the People's Republic of China. National Geological Disaster Bulletin. 2016. Available online: <http://cigem.cn/auto/db/detail.aspx?db=1006&rid=35360&md=15&pd=210&msd=11&psd=5&mdd=11&pdd=5&count=20> (accessed on 22 February 2017).
9. Zhu, D.; Ren, G.; Nie, D.; Ge, X. Effecting and Forecasting of Landslide Stability with the Change of Reservoir Water Level. *Hydrogeol. Eng. Geol.* **2002**, *3*, 6–9. [CrossRef]
10. Zhou, J.; Chen, M.; Li, H.; Xu, N.; Xiao, M.; Yang, X.; Sun, H.; Qi, S. Formation and movement mechanisms of water-induced landslides and hazard prevention and mitigation technologies. *J. Eng. Geol.* **2019**, *27*, 1131–1145. [CrossRef]
11. WANG, R.; Xia, R.; XU, W.; WANG, H.; QI, J. Study on Physical Simulation of Rainfall Infiltration Process of Landslide Accumulation Body. *Adv. Eng. Sci.* **2019**, *51*, 47–54. [CrossRef]
12. Liao, H.; Sheng, Q.; Gao, S.; Xu, Z. Influence of Drawdown of Reservoir Water Level on Landslide Stability. *Chin. J. Rock Mech. Eng.* **2005**, *24*, 3454–3458. [CrossRef]
13. Wu, L.; Zhang, Y.; Xie, W.; Li, Y.; Song, J. Summary of Remote Sensing Methods for Monitoring Soil Moisture. *Remote Sens. LANDResour.* **2014**, *26*, 19–26. [CrossRef]
14. Dasberg, S.; Dalton, F.N. Time Domain Reflectometry Field Measurements of Soil Water Content and Electrical Conductivity. *Soil Sci. Soc. Am. J.* **1985**, *49*, 293–297. [CrossRef]
15. Skierucha, W.; Wilczek, A.; Alokchina, O. Calibration of a TDR Probe for Low Soil Water Content Measurements. *Sens. Actuators A. Phys.* **2008**, *147*, 544–552. [CrossRef]
16. Skierucha, W. Accuracy of Soil Moisture Measurement by Tdr Technique. *Int. Agrophys.* **2000**, *14*, 417–426.
17. Leng, Y.; Lin, H.; Liu, C.; Qiao, J. Analysis on Calibration Tests for TDR Moisture Meter. *Geotech. Investig. Surv.* **2014**, *42*, 1–4+16. [CrossRef]
18. Zhang, X.; Hu, Z.; Chu, S. Methods for Measuring Soil Water Content: A Review. *Chin. J. Soil Sci.* **2005**, *36*, 118–123. [CrossRef]

19. Gao, L.; Shi, B.; Tang, C.; Wang, B.; Gu, K.; Gan, Y. Experimental Study of Temperature Effect on FDR Measured Soil Volumetric Water Content. *J. Glaciol. Geocryol.* **2010**, *32*, 964–969.
20. Feng, C. Application of the Neutron Meter in Construction of Farmland and Soil Improvement. *Nucl. Electron. Detect. Technol.* **1992**, *12*, 288–294.
21. Li, J. A Generalized Description of the Development of Electric Exploration Methods. *Geophys. Geochem. Explor.* **1996**, *20*, 250–258+249.
22. LI, Z. Development of High Density Electro-Mechanical Instruments. *Geol. Equip.* **2013**, *14*, 25–29. [[CrossRef](#)]
23. Dai, Q.; Tai, X.; Wang, P. Comparative Analysis of Model Response Based on Ultra-High Density Resistivity Method. *Chin. J. Eng. Geophys.* **2013**, *10*, 383–388. [[CrossRef](#)]
24. YAN, J.; MENG, G.; LV, Q.; ZHANG, K.; CHEN, X. The Progress and Prospect of the Electrical Resistivity Imaging Survey. *Geophys. Geochem. Explor.* **2012**, *36*, 576–584.
25. Yu, W.; Liao, Y.; He, F. High-Density Resistivity Method in the Application of Cultural Relics and Archeology. *Chin. J. Eng. Geophys.* **2009**, *6*, 91–94. [[CrossRef](#)]
26. Di, Q.; Ni, D.; Wang, R.; Wang, M. High-Density Resistivity Image. *Prog. Geophys.* **2003**, *02*, 323–326. [[CrossRef](#)]
27. Jiang, Z.; Bian, J.; Zha, E.; Lin, N.; Tian, W. The Application of the Electrical Resistivity Tomography in Hydrology: An Overview. *Hydrogeol. Eng. Geol.* **2010**, *37*, 21–26. [[CrossRef](#)]
28. Samouëlian, A.; Cousin, I.; Tabbagh, A.; Bruand, A.; Richard, G. Electrical Resistivity Survey in Soil Science: A Review. *Soil Tillage Res.* **2004**, *83*, 173–193. [[CrossRef](#)]
29. Chu, X.; Liu, S.; Wang, L.; Xu, W.; Wang, J. Influences of Water Content and Potential Gradient on Electrical Resistivity of Soil in Electro-Osmosis Method. *J. Hohai Univ. Sci.* **2010**, *38*, 575–579. [[CrossRef](#)]
30. Masaki, H. Temperature-Electrical Conductivity Relation of Water for Environmental Monitoring and Geophysical Data Inversion. *Environ. Monit. Assess.* **2004**, *96*, 119–128.

Disclaimer/Publisher’s Note: The statements, opinions and data contained in all publications are solely those of the individual author(s) and contributor(s) and not of MDPI and/or the editor(s). MDPI and/or the editor(s) disclaim responsibility for any injury to people or property resulting from any ideas, methods, instructions or products referred to in the content.